Fillowite, $Na_2Ca(Mn,Fe)_7^{2+}(PO_4)_6$: its crystal structure

TAKAHARU ARAKI AND PAUL B. MOORE

Department of the Geophysical Sciences
The University of Chicago
Chicago, Illinois 60637

Abstract

Fillowite, $Na_2Ca(Mn,Fe)_7^{2+}(PO_4)_6$, possesses a structure derived from the glaserite, $K_3Na(SO_4)_2$, arrangement. No evidence of substructure occurs either in the X-ray data or the polyhedral arrangement. It is rhombohedral, a_1 15.282(2), c 43.507(3)Å, $Z = 18$, space group $R\overline{3}$. $R = 0.069$ for 6891 independent reflections. Forty-five nonequivalent atoms occur in the asymmetric unit. Nine distinct MO_6 octahedra, four distinct five-coordinate polyhedra, one seven-coordinate polyhedron, one eight-coordinate polyhedron and six distinct PO_4 tetrahedra occur in the asymmetric unit. The eight-coordinate polyhedron, maximal point symmetry $\overline{4}m2$, is the *gable disphenoid* and is identical to a polyhedron in the related mineral wyllieite, $Na_2Fe_2^{2+}Al(PO_4)_3$. In these structures, the ratio of larger cations to tetrahedra is $X:T = 5:3$.

Three kinds of rods occur in the structure and, when projected down the c-axis, define the regular $\{6^3\}$ hexagonal tessellation. Rod I at the origin has the cation sequence $\cdots$ M(1)–M(3)–Na(1)–Na(2)–M(4)–M(5)–M(2)–M(5)–M(4)–Na(2)–Na(1)–M(3) $\cdots$ with five octahedra in sequence sharing faces: M(3)–Na(1)–Na(2)–M(4)–M(5). Rod II along the 3_1-axis has $\cdots$ Ca–M(9)–Na(3)–M(8)–Ca–M(9)–Na(3)–M(8)–Ca–M(9)–Na(3)–M(8) $\cdots$ Rod III at the nodes of the hexagonal net includes the six nonequivalent PO_4 tetrahedra, $\cdots$ P(6)–M(11)–P(4)–M(6)–P(1)–□(1)–P(5)–M(7)–P(2)–M(10)–P(3)–□(2) $\cdots$. Counting up the cations, the ratio of larger cations (X) to tetrahedra (T) is $\square_8X_{40}T_{24}$ or $X:T = 5:3$.

Introduction

Fillowite is an exceedingly complex mineral which occurs as a primary accessory phosphate phase in granitic pegmatites. Its high specific gravity, granular character, colors ranging from orange in the Mn-rich member to reddish-brown in the Fe-rich member (johnsomervilleite) and uncanny physical similarity to phases like triploidite, griphite, graftonite and spessartine render it an unusually difficult phase to identify in the field. Occurrences of the mineral include the type locality at Branchville, Connecticut (Brush and Dana, 1878); Kabira, Uganda (Von Knorring, 1963); Inverness-shire, Scotland (Livingstone, 1980) and a new locality noted by one of us (PBM) at the Sapucaia pegmatite, State of Minas Gerais, Brazil where the mineral occurs locally as abundant metamict nodules whose single crystal character was restored upon heating in air at 500°C for two days. The type occurrence and the Uganda locality are the only ones representing the Mn-predominant member, hence fillowites, while the remaining are Fe-predominant, hence johnsomervilleites. All indications presently at hand suggest that the fillowite series is confined to a primary, high temperature pegmatite assemblage and the series may in fact be far more abundant than hitherto noted.

Fillowite has been a subject of ongoing controversy concerning its crystal chemistry. Brush and Dana (1890) concluded that fillowite is morphologically related to dickinsonite which presents, on morphological and chemical grounds, an interesting case of dimorphism. They proposed the formula $X_3P_2O_8 \cdot 1/3H_2O$ where $X = $ large cations, or $H_4X_{36}(PO_4)_{24} \cdot 2H_2O$. Palache *et al.* (1951) proposed $H_4Na_{12}(Mn,Fe,Ca)_{28}(PO_4)_{24} \cdot 2H_2O$. Fisher (1965) in an exhaustive study on the alluaudite, arrojadite and fillowite species proposed (after our scaling) $Ca_{2.8}Na_{7.67}Mn_{23.6\,8}Fe_{5.\,6}(PO_4)_{24}$ or $X_{40}(PO_4)_{24}$. Strunz (1970) and Povarennykh (1972) offer $Na_{12}Mn_{30}(PO_4)_{24}$ or $X_{42}(PO_4)_{24}$. Our structure study shows that by counting atoms, the idealized formula for fillowite

is $Na_8Ca_4Mn_{28}^{2+}(PO_4)_{24}$ or $X_{40}(PO_4)_{24}$, bearing in mind that substantial solid solution of (Na,Ca,Mn), (Mn,Fe,Ca) and (Mn,Na) does not admit statement of a precise end-member formula.

Experimental

Crystals of fillowite were obtained from one of the Brush–Dana cotypes housed in the Harvard University Mineralogical Museum, HMM96840. The crystal measured 0.15 mm ($11a_1$) × 0.47 mm ($11a_2$) × 0.28 mm ($11c$). The crystal cell parameters were obtained using calibrated precession photographs (then refined from the orientation matrix) and MoK_α radiation; the results are a_1 15.282(2), c 43.507(3)Å. Data were collected on a Picker four-circle diffractometer with the a_2-axis parallel to the ϕ axis of the machine. The ω-scan had constant 2.6° width. Utilizing monochromatized MoK_α radiation, data were collected for (hk$l$) and (hk$\bar{l}$), and up to sin $\theta/\lambda = 0.75$. A total of 7567 reflections were collected, with 730 unobserved as $I < 2\sigma(I)$ and these were reset to $I = \sigma(I)$. Absorption corrections used the Gaussian integral method with 10 planes approximating the crystal shape. Extremes in the transmission factor ranged between 0.196 and 0.310. Centric tests, including N(z) and E_0 statistics supported the centric $R\bar{3}$ space group, as did the final structure refinement. After averaging equivalent reflections, 6891 unique $|F_0|$ remained.

The structure was solved with difficulty from the Patterson synthesis. We used scattering curves for Ca^{2+}, Mn^{2+}, Fe^{2+}, Na^{1+}, P^{5+} and O^{1-} from Cromer and Mann (1968), and anomalous dispersion corrections for Ca, Mn, Fe and P from Cromer and Liberman (1970). Full-matric anisotropic least-squares refinement for 6891 $|F_0|$ and 368 variable parameters converged to

$$R = \frac{\| F_0| - |F_c \|}{\sum F_0} = 0.069$$

$$R_w = \left[\frac{\sum_\omega (|F_0| - |F_c|)^2}{\sum_\omega F_0^2} \right]^{1/2} = 0.062.$$

The final cycle minimized $\sum_\omega \| F_0| - |F_c \|^2$ where $\omega = \sigma^{-2}(F)$.

The final atomic coordinate parameters for fillowite are given in Table 1. Table 2 presents the anisotropic thermal vibration parameters, Table 3, the parameters for ellipsoids of vibration and Table 4 the

Table 1. Fillowite atomic coordinate parameters†

Atom	x	y	z	Atom	x	y	z
M(1)	0	0	0	P(3)	0.54217(8)	0.09121(8)	0.19936(2)
M(2)	0	0	½	O(9)	0.54102(25)	0.03154(25)	0.17097(7)
M(3)	0	0	0.10083(2)	O(10)	0.62717(24)	0.20328(24)	0.19749(7)
M(4)	0	0	0.32463(2)	O(11)	0.43952(24)	0.08876(25)	0.20189(7)
M(5)	0	0	0.39880(3)	O(12)	0.55031(25)	0.04003(25)	0.22916(7)
M(6)	0.42839(5)	0.24706(6)	0.05159(1)				
M(7)	0.11125(5)	0.57169(6)	0.03778(1)	P(4)	0.21794(9)	0.12273(8)	0.20976(2)
M(8)	0.00343(5)	0.32387(5)	0.08210(1)	O(13)	0.23250(29)	0.07960(28)	0.17998(7)
M(9)	0.26360(5)	0.33025(5)	0.08576(1)	O(14)	0.12532(25)	0.13521(25)	0.20748(8)
M(10)	0.57395(5)	0.08154(5)	0.12440(2)	O(15)	-0.11095(24)	0.23987(24)	0.11603(7)
M(11)	0.22241(5)	0.10811(5)	0.13377(2)	O(16)	0.19863(27)	0.04226(25)	0.23476(7)
Na(1)	0	0	0.17485(7)				
Na(2)	0	0	0.24871(8)	P(5)	0.22502(8)	0.46060(8)	0.22200(2)
Na(3)	0.07920(19)	0.42728(19)	0.16515(5)	O(17)	0.27073(29)	0.52738(26)	0.19431(7)
Ca	0.26607(11)	0.29074(10)	0.00104(3)	O(18)	0.10715(24)	0.40130(25)	0.21959(7)
				O(19)	0.25370(25)	0.37674(24)	0.22244(7)
P(1)	0.19099(8)	0.43418(8)	0.02780(2)	O(20)	0.25286(25)	0.51960(23)	0.25266(7)
O(1)	0.16384(24)	0.38196(24)	-0.00371(7)				
O(2)	0.25347(25)	0.55116(23)	0.02559(7)	P(6)	0.46755(9)	0.21656(9)	0.27903(2)
O(3)	0.25597(25)	0.39869(26)	0.04487(7)	O(21)	0.52428(25)	0.24646(27)	0.24824(8)
O(4)	0.09274(25)	0.41058(26)	0.04415(7)	O(22)	0.38217(24)	0.10219(25)	0.27484(7)
				O(23)	0.41433(27)	0.27752(27)	0.28429(7)
P(2)	0.53388(9)	0.11487(8)	0.03893(2)	O(24)	0.53077(30)	0.22013(31)	0.30646(9)
O(5)	0.46016(25)	0.12678(25)	0.06001(7)				
O(6)	0.55695(26)	0.03458(25)	0.05085(7)				
O(7)	0.63683(25)	0.21482(24)	0.03920(7)				
O(8)	0.48812(30)	0.09088(27)	0.00646(7)				

†Estimated standard errors refer to the last digit.

Table 2. Fillowite: anisotropic thermal vibration parameters†

	U_{11}	U_{22}	U_{33}	U_{12}	U_{13}	U_{23}
M(1)	95(8)	95	126(8)	47	0	0
M(2)	96(6)	96	106(6)	48	0	0
M(3)	108(5)	108	152(5)	54	0	0
M(4)	117(5)	117	119(5)	58	0	0
M(5)	95(5)	95	135(5)	47	0	0
M(6)	110(3)	175(3)	118(3)	78(3)	0(2)	−9(2)
M(7)	99(3)	184(3)	107(3)	79(3)	−7(2)	1(2)
M(8)	97(3)	107(3)	128(3)	42(2)	9(2)	10(2)
M(9)	114(3)	104(3)	103(3)	51(3)	0(2)	−2(2)
M(10)	137(3)	76(3)	192(3)	45(3)	53(3)	17(2)
M(11)	121(3)	91(3)	177(3)	60(3)	41(2)	17(2)
Na(1)	199(20)	199	165(17)	100	0	0
Na(2)	326(26)	326	216(20)	163	0	0
Na(3)	391(14)	350(13)	194(9)	288(12)	32(9)	69(9)
Ca	340(8)	288(7)	154(6)	279(6)	−37(5)	−29(5)
P(1)	70(4)	75(4)	82(4)	34(4)	3(3)	4(3)
O(1)	120(14)	107(14)	105(12)	44(4)	−23(11)	−24(11)
O(2)	165(16)	59(13)	115(13)	−3(12)	16(11)	−8(11)
O(3)	137(15)	203(17)	139(13)	131(14)	17(11)	42(12)
O(4)	106(14)	194(17)	150(14)	86(13)	40(11)	27(12)
P(2)	119(5)	69(5)	107(4)	40(4)	13(4)	1(3)
O(5)	144(16)	115(15)	170(15)	52(13)	86(12)	10(12)
O(6)	189(17)	108(15)	209(16)	92(13)	−47(13)	7(12)
O(7)	130(15)	91(14)	215(16)	59(13)	27(12)	31(12)
O(8)	286(20)	181(17)	132(14)	132(15)	−21(13)	−25(12)
P(3)	81(5)	70(4)	106(4)	34(4)	1(4)	−2(3)
O(9)	150(15)	107(14)	134(13)	49(12)	10(11)	−27(11)
O(10)	115(14)	74(13)	162(14)	36(12)	19(11)	−4(11)
O(11)	103(14)	140(15)	150(14)	71(12)	17(11)	35(11)
O(12)	130(15)	130(15)	147(14)	78(13)	−12(11)	28(11)
P(4)	102(5)	80(5)	112(4)	47(4)	−29(4)	−21(4)
O(13)	274(20)	235(19)	132(15)	153(16)	−14(13)	−57(13)
O(14)	108(15)	124(15)	282(17)	66(13)	−62(13)	−47(13)
O(15)	81(14)	123(14)	162(14)	54(12)	44(11)	38(11)
O(16)	198(17)	105(15)	135(14)	74(13)	−31(12)	1(11)
P(5)	76(4)	71(4)	78(4)	33(4)	−1(3)	2(3)
O(17)	263(19)	129(16)	144(14)	89(15)	70(13)	67(12)
O(18)	72(14)	141(15)	170(15)	37(12)	−14(11)	−39(12)
O(19)	127(15)	119(15)	140(14)	79(12)	−32(11)	−11(11)
O(20)	154(15)	89(14)	120(13)	53(12)	−13(11)	−29(11)
P(6)	99(5)	106(5)	115(4)	62(4)	2(4)	−12(4)
O(21)	121(16)	178(17)	189(15)	32(13)	72(12)	−8(13)
O(22)	111(15)	108(15)	187(15)	38(12)	21(12)	−20(12)
O(23)	206(17)	195(17)	180(15)	168(15)	36(13)	6(13)
O(24)	264(20)	287(21)	284(19)	187(18)	−156(16)	−97(16)

†Coefficients in the expression exp−[$U_{11}h^2 + U_{22}k^2 + U_{33}l^2 + 2U_{12}hk + 2U_{13}hl + 2U_{23}kl$]. Estimated standard errors refer to the last digit except for those coefficients related by symmetry.

observed and calculated structure factors.[1] The bond distance and angle calculations are given in Table 5, and Table 6 lists some characteristics of the 15 discrete larger cation polyhedra.

The scattering curves indicated for each larger cation site and summarized in Table 6 were initially selected by the relative heights on the final Fourier synthesis, the coordination number and polyhedral type, and mean cation–anion bond distances and thermal vibration parameters. The sites M(1), Na(1), Na(2) and Ca were refined involving more than one curve. The decisions on M(2) through M(11) occupancies were admittedly guided by bond distances since Mn^{2+} and Fe^{2+} cannot be easily distinguished by site refinement. For M(8), $2/3Fe^{2+} + 1/3Mn^{2+}$

[1] To obtain a copy of Table 4, order Document AM-81-161 from the Business Office, Mineralogical Society of America, 2000 Florida Avenue, N.W., Washington, D.C. 20009. Please remit $1.00 in advance for the microfiche.
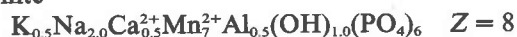
were locked in, suggested by the mean bond distance. M(3) almost certainly includes some Mn^{2+} as well but the remainder have mean bond distances expected for their cations and coordination numbers. The final M(1)–M(11) equivalent isotropic thermal vibration parameters range from 0.8–1.1$Å^2$, and those for Na(1)–Ca from 1.5–2.3$Å^2$, typical values for these cations in related structures, and suggest that departures from Table 6 are probably not serious.

Description of the structure

Fillowite is one of the most elaborate examples of a mineral structure. It contains 45 nonequivalent atoms in the asymmetric unit of structure, some of which constitute remarkable coordination polyhedra. Neither single crystal photographs nor the structure itself indicate any pseudosymmetry. As we shall see, the structure type is pseudo-dimorphous to dickinsonite and as both structures are known, the hypothetical end-member formulas can be written.

fillowite $\quad Na_2CaMn_7^{2+}(PO_4)_6 \quad Z = 18$

dickinsonite

$$K_{0.5}Na_{2.0}Ca_{0.5}^{2+}Mn_7^{2+}Al_{0.5}(OH)_{1.0}(PO_4)_6 \quad Z = 8$$

These constitute ideal end-member formulae and show that fillowite contains essential Ca^{2+} (which resides in a *gable disphenoid*) and that dickinsonite possesses essential K^+ and Al^{3+} in cubic and octahedral coordination respectively, with an additional $(OH)^-$ ligand. Detailed comparison of the two structure types will be deferred to the future paper on dickinsonite. Suffice it to say that the principal polyhedral rods in the two structures are similar but that the two structures are based on different kinds of plane nets normal to the rods (Moore, 1981).

Chemical analyses and computed analyses for the formulae $Na_3CaMn_{11}^{2+}(PO_4)_9$ and $Na_2CaMn_7^{2+}(PO_4)_6$ appear in Table 7. Some ambiguity exists with regard to a true end-member formula owing to some solid solution among Na, Ca and Mn. The second formula, which is favored in this study, agrees well with the recent chemical analyses on the Fe-analogue johnsomervilleite both done by electron microprobe analysis and differs only from the original analytic results on type material in containing somewhat more Ca, no water, and no extraneous phase.

Table 6 outlines the cationic species, their equipoint rank numbers (ERN), coordination numbers (C · N ·) by oxyanions, the average cation (X)–oxygen bond length, the scattering curve used, followed by two important kinds of distances. The first

Table 3. Fillowite: parameters for the ellipsoids of vibration†

Atom	i	μ_i	θ_{ia}	θ_{ib}	θ_{ic}	Beq., Å²	Atom	i	μ_i	θ_{ia}	θ_{ib}	θ_{ic}	Beq., Å²
M(1)	1	0.097(6)	···not determined···			0.83(5)	O(6)	1	0.086(8)	56(18)	163(61)	73(11)	1.27(5)
	2	0.097	···not determined···					2	0.125(6)	125(10)	104(8)	123(7)	
	3	0.112(4)	90	90	0			3	0.159(5)	127(7)	8C(5)	38(9)	
M(2)	1	0.098(4)	···not determined···			0.78(3)	O(7)	1	0.089(8)	74(16)	163(52)	79(7)	1.13(5)
	2	0.098	···not determined···					2	0.112(7)	19(47)	106(17)	103(10)	
	3	0.103(3)	90	90	0			3	0.150(5)	81(7)	83(5)	17(8)	
M(3)	1	0.104(3)	···not determined···			0.97(2)	O(8)	1	0.110(7)	95(8)	65(15)	26(11)	1.52(6)
	2	0.104	···not determined···					2	0.130(6)	116(11)	25(32)	115(22)	
	3	0.123(2)	90	90	0			3	0.170(6)	154(15)	85(7)	83(5)	
M(4)	1	0.108(3)	···not determined···			0.93(2)	P(3)	1	0.084(3)	86(13)	34(27)	88(5)	0.69(1)
	2	0.108	···not determined···					2	0.093(2)	6(90)	124(64)	95(18)	
	3	0.109(2)	90	90	0			3	0.103(2)	85(10)	95(7)	5(2)	
M(5)	1	0.097(3)	···not determined···			0.85(2)	O(9)	1	0.094(7)	98(10)	40(11)	55(15)	1.08(5)
	2	0.097	···not determined···					2	0.116(6)	57(14)	78(12)	129(14)	
	3	0.116(2)	90	90	0			3	0.138(6)	34(33)	127(20)	59(20)	
M(6)	1	0.099(2)	165(59)	67(8)	77(10)	1.04(1)	O(10)	1	0.086(8)	90(13)	30(27)	87(9)	0.96(5)
	2	0.108(1)	102(7)	93(3)	164(6)			2	0.108(6)	28(29)	115(18)	118(18)	
	3	0.134(1)	81(7)	157(8)	81(3)			3	0.132(6)	62(13)	105(8)	28(12)	
M(7)	1	0.091(2)	21(16)	111(3)	70(7)	1.00(1)	O(11)	1	0.095(7)	1(90)	121(90)	89(36)	1.00(5)
	2	0.105(1)	71(5)	95(2)	160(3)			2	0.105(7)	89(31)	50(33)	131(15)	
	3	0.136(1)	99(2)	22(25)	88(2)			3	0.134(6)	90(7)	55(10)	41(10)	
M(8)	1	0.096(1)	129(7)	108(4)	74(3)	0.90(1)	O(12)	1	0.089(7)	46(23)	141(28)	59(16)	1.03(5)
	2	0.109(1)	141(38)	28(54)	106(18)			2	0.117(6)	49(26)	72(20)	99(13)	
	3	0.115(1)	93(8)	69(10)	22(4)			3	0.132(6)	108(16)	57(11)	33(20)	
M(9)	1	0.101(1)	92(8)	58(34)	36(34)	0.86(1)	P(4)	1	0.083(3)	84(10)	45(18)	62(4)	0.77(2)
	2	0.103(1)	82(9)	51(27)	125(29)			2	0.093(2)	147(29)	45(18)	116(14)	
	3	0.109(1)	8(90)	125(44)	84(14)			3	0.117(2)	122(5)	92(4)	40(4)	
M(10)	1	0.086(2)	90(3)	150(6)	82(2)	1.10(1)	O(13)	1	0.099(7)	103(6)	61(7)	30(6)	1.59(6)
	2	0.107(1)	33(5)	118(4)	123(3)			2	0.149(6)	139(24)	37(28)	116(14)	
	3	0.151(1)	57(1)	100(1)	34(1)			3	0.169(6)	128(22)	110(9)	78(5)	
M(11)	1	0.091(2)	123(38)	5(90)	86(7)	1.00(1)	O(14)	1	0.092(8)	19(72)	108(28)	75(7)	1.32(5)
	2	0.099(1)	43(10)	86(8)	118(3)			2	0.106(7)	75(25)	161(60)	101(8)	
	3	0.141(1)	65(1)	92(1)	28(1)			3	0.175(5)	102(3)	97(4)	19(5)	
Na(1)	1	0.128(6)	90	90	0	1.48(12)	O(15)	1	0.078(5)	82(11)	43(14)	68(7)	0.95(5)
	2	0.141(10)	···not determined···					2	0.105(7)	20(50)	118(18)	110(16)	
	3	0.141	···not determined···					3	0.138(5)	72(9)	120(8)	31(9)	
Na(2)	1	0.147(7)	90	90	0	2.29(15)	O(16)	1	0.098(7)	71(19)	158(84)	72(31)	1.16(5)
	2	0.181(10)	···not determined···					2	0.111(6)	106(11)	102(21)	150(20)	
	3	0.181	···not determined···					3	0.149(6)	154(20)	74(7)	67(10)	
Na(3)	1	0.114(4)	54(6)	139(9)	53(8)	2.10(4)	P(5)	1	0.084(3)	106(25)	133(39)	81(20)	0.61(1)
	2	0.146(4)	52(6)	119(6)	140(6)			2	0.088(2)	117(33)	78(30)	153(28)	
	3	0.213(3)	58(4)	64(2)	78(2)			3	0.091(2)	148(90)	46(72)	65(56)	
Ca	1	0.082(3)	35(75)	155(90)	87(5)	1.63(3)	O(17)	1	0.083(8)	92(4)	128(7)	47(5)	1.45(5)
	2	0.122(2)	93(2)	96(3)	171(1)			2	0.134(6)	63(8)	140(9)	130(9)	
	3	0.201(2)	125(2)	114(1)	81(1)			3	0.174(6)	27(13)	102(6)	69(6)	
P(1)	1	0.083(3)	135(44)	103(22)	76(12)	0.60(1)	O(18)	1	0.084(8)	34(19)	87(8)	81(7)	1.06(5)
	2	0.088(3)	135(87)	24(90)	107(54)			2	0.114(6)	60(13)	138(13)	130(14)	
	3	0.091(2)	92(23)	70(30)	23(17)			3	0.143(6)	75(7)	131(12)	42(10)	
O(1)	1	0.088(7)	135(15)	74(11)	46(15)	0.92(5)	O(19)	1	0.090(7)	32(68)	139(46)	68(25)	0.96(5)
	2	0.114(6)	128(40)	92(51)	133(37)			2	0.108(6)	98(15)	130(23)	123(13)	
	3	0.119(6)	70(72)	164(90)	77(60)			3	0.129(6)	121(8)	95(10)	41(14)	
O(2)	1	0.072(9)	79(8)	41(38)	87(8)	1.10(5)	O(20)	1	0.084(8)	96(7)	38(12)	59(10)	0.98(5)
	2	0.106(6)	80(5)	94(8)	170(8)			2	0.117(6)	98(25)	60(17)	149(15)	
	3	0.160(6)	15(90)	130(22)	80(9)			3	0.129(6)	171(90)	69(47)	86(30)	
O(3)	1	0.080(8)	22(90)	136(44)	77(18)	1.10(5)	P(6)	1	0.087(3)	147(29)	38(26)	70(10)	0.80(1)
	2	0.112(6)	71(10)	83(8)	152(8)			2	0.103(2)	122(9)	111(10)	116(10)	
	3	0.152(6)	79(4)	47(7)	66(6)			3	0.111(2)	87(8)	120(6)	34(14)	
O(4)	1	0.086(8)	152(17)	73(7)	65(9)	1.14(5)	O(21)	1	0.086(8)	137(5)	90(5)	58(6)	1.43(5)
	2	0.124(6)	117(10)	55(15)	142(15)			2	0.132(6)	88(7)	135(9)	127(7)	
	3	0.144(6)	89(8)	40(17)	64(11)			3	0.172(6)	47(11)	135(13)	53(11)	
P(2)	1	0.082(3)	97(8)	23(90)	89(7)	0.80(2)	O(22)	1	0.099(7)	63(90)	57(90)	89(11)	1.13(5)
	2	0.100(2)	63(6)	99(7)	153(6)			2	0.109(7)	40(53)	135(50)	121(28)	
	3	0.117(2)	28(14)	111(5)	63(8)			3	0.146(5)	63(9)	116(9)	31(11)	
O(5)	1	0.083(8)	134(11)	82(13)	48(10)	1.18(5)	O(23)	1	0.075(9)	147(36)	32(35)	76(10)	1.29(5)
	2	0.109(7)	79(13)	159(57)	99(13)			2	0.133(6)	91(7)	69(7)	156(11)	
	3	0.161(5)	46(7)	109(6)	44(6)			3	0.160(6)	57(7)	67(8)	70(8)	
							O(24)	1	0.104(8)	38(11)	107(8)	52(5)	2.02(7)
								2	0.146(5)	65(8)	157(10)	113(8)	
								3	0.211(6)	117(3)	105(4)	47(4)	

†i = ith principal axis, μ_i'= rms amplitude, θ_{ia}, θ_{ib}, θ_{ic} = angles (deg.) between the ith principal axis and the cell axes a_1, a_2 and c. The equivalent isotropic thermal parameter, $B_{eq.}$, is also listed. Estimated standard errors in parentheses refer to the last digit.

Table 5. Fillowite: bond distances and angles†

M(1)

6 M(1)-O(24)[(4a)]	2.254(4) Å	
		Angle (°)
6 O(24)[(4a)]-O(24)[(3b)]	3.030(6)	84.5(1)
6 O(24)[(4a)]-O(24)[(5a)]	3.337(7)	95.5(1)
Average	3.184	90.0

M(2)

6 M(2)-O(17)[(2a)]	2.204(3)	
6 O(17)[(2a)]-O(17)[(4b)]	3.033(5)**	87.0(1)
6 O(17)[(2a)]-O(17)[(3a)]	3.198(6)	93.0(1)
Average	3.116	90.0

M(3)

3 M(3)-O(21)[(4a)]	2.019(3)	
3 M(3)-O(10)[(4a)]	2.331(3)	
Average	2.175	
3 O(10)[(4a)]-O(21)[(5a)]	2.775(5)	78.9(1)
3 O(10)[(4a)]-O(21)[(4a)]	2.970(4)**	85.8(1)
3 O(10)[(4a)]-O(10)[(5a)]	3.057(5)**	81.9(1)
3 O(21)[(4a)]-O(21)[(5a)]	3.290(6)	109.1(1)
Average	3.023	88.9

M(4)

3 M(4)-O(7)[(4a)]	2.103(3)	
3 M(4)-O(2)[(1a)]	2.163(3)	
Average	2.133	
3 O(2)[(1a)]-O(2)[(2a)]	2.712(5)**	77.6(1)
3 O(7)[(4a)]-O(7)[(5a)]	2.826(6)**	84.4(1)
3 O(2)[(1a)]-O(7)[(5a)]	2.950(4)	87.6(1)
3 O(2)[(1a)]-O(7)[(6a)]	3.595(5)	114.8(1)
Average	3.021	91.1

M(5)

3 M(5)-O(20)[(4b)]	2.058(3)	
3 M(5)-O(2)[(2a)]	2.337(3)	
Average	2.198	
3 O(2)[(2a)]-O(2)[(3a)]	2.712(5)**	70.9(1)
3 O(2)[(3a)]-O(20)[(4b)]	2.851(4)**	80.6(1)
3 O(2)[(2a)]-O(20)[(4b)]	3.137(4)	90.9(1)
3 O(20)[(4b)]-O(20)[(5b)]	3.376(5)	110.2(1)
Average	3.019	88.2

M(6)

M(6)-O(22)[(4a)]	2.110(3)	
M(6)-O(16)[(4a)]	2.142(3)	
M(6)-O(7)[(3)]	2.147(3)	
M(6)-O(5)[(1)]	2.154(4)	
M(6)-O(1)[(5)]	2.174(3)	
Average	2.145	
O(1)[(5)]-O(22)[(4a)]	2.870(4)**	84.1(1)
O(5)[(1)]-O(16)[(4a)]	2.972(5)	87.5(1)
O(7)[(3)]-O(16)[(4a)]	2.976(5)	87.9(1)
O(16)[(4a)]-O(22)[(4a)]	3.030(5)	90.9(1)
O(1)[(5)]-O(7)[(3)]	3.103(5)	91.8(1)
O(5)[(1)]-O(7)[(3)]	3.257(5)	98.4(1)
O(1)[(5)]-O(5)[(1)]	3.323(5)	100.3(1)
O(5)[(1)]-O(22)[(4a)]	3.747(5)	123.0(1)
Average	3.160	95.5

M(7)

M(7)-O(8)[(5)]	2.043(3)	
M(7)-O(6)[(2)]	2.044(3)	
M(7)-O(20)[(5a)]	2.119(3)	
M(7)-O(4)[(1)]	2.350(4)	
M(7)-O(2)[(1)]	2.405(4)	
M(7)-O(3)[(3)]	2.449(4)	
Average	2.235	
O(2)[(1)]-O(4)[(1)]	2.454(5)*	62.1(1)
O(2)[(1)]-O(20)[(5a)]	2.851(4)**	77.8(1)
O(3)[(3)]-O(8)[(5)]	2.926(5)**	80.8(1)
O(4)[(1)]-O(2)[(5a)]	2.969(5)	83.1(1)
O(6)[(2)]-O(8)[(5)]	3.008(5)	94.8(1)
O(3)[(3)]-O(20)[(5a)]	3.029(5)	82.8(1)
O(3)[(3)]-O(6)[(2)]	3.115(5)	87.3(1)
O(4)[(1)]-O(6)[(2)]	3.180(5)	92.5(1)
O(6)[(2)]-O(20)[(5a)]	3.237(5)	102.1(1)
O(2)[(1)]-O(8)[(5)]	3.271(5)	94.3(1)
O(4)[(1)]-O(8)[(5)]	3.682(5)	113.7(1)
O(2)[(1)]-O(3)[(3)]	>3.75 Å	117.6(1)
Average	>3.122	90.7

M(8)

M(8)-O(4)[(1)]	2.130(3)	
M(8)-O(15)[(1)]	2.154(3)	
M(8)-O(19)[(5a)]	2.192(3)	
M(8)-O(23)[(5a)]	2.217(3)	
M(8)-O(12)[(4a)]	2.219(3)	
M(8)-O(5)[(2)]	2.279(3)	
Average	2.198	
O(5)[(2)]-O(23)[(5a)]	2.837(5)	78.2(1)
O(5)[(2)]-O(15)[(1)]	2.896(4)	81.5(1)
O(4)[(1)]-O(23)[(5a)]	2.911(5)**	84.1(1)
O(15)[(1)]-O(19)[(5a)]	2.959(5)	85.8(1)
O(4)[(1)]-O(5)[(2)]	3.027(5)	86.7(1)
O(4)[(1)]-O(19)[(5a)]	3.165(4)	94.2(1)
O(12)[(4a)]-O(15)[(1)]	3.188(5)	93.6(1)
O(15)[(1)]-O(23)[(5a)]	3.194(5)	93.9(1)
O(5)[(2)]-O(19)[(5a)]	3.211(4)	91.8(1)
O(12)[(4a)]-O(19)[(5a)]	3.212(5)	93.5(1)
O(4)[(1)]-O(12)[(4a)]	3.287(4)	98.2(1)
O(12)[(4a)]-O(23)[(5a)]	3.313(5)	96.6(1)
Average	3.100	89.8

M(9)

M(9)-O(18)[(5a)]	2.070(3)	
M(9)-O(22)[(4a)]	2.071(3)	
M(9)-O(3)[(1)]	2.096(3)	
M(9)-O(12)[(4a)]	2.180(3)	
M(9)-O(11)[(4a)]	2.290(3)	
Average	2.141	

Apical edges

O(11)[(4a)]-O(12)[(4a)]	2.468(4)*	67.0(1)
O(11)[(4a)]-O(18)[(6a)]	2.800(4)**	79.7(1)
O(3)[(1)]-O(22)[(4a)]	2.866(5)**	86.9(1)
O(3)[(1)]-O(12)[(4a)]	3.220(4)	97.7(1)
O(11)[(4a)]-O(22)[(4a)]	3.327(5)	99.3(1)
O(3)[(1)]-O(18)[(6a)]	3.380(4)	108.4(1)
Average	3.010	89.8

Meridional edges

O(12)[(4a)]-O(18)[(6a)]	3.428(5)	107.5(1)
O(18)[(6a)]-O(22)[(4a)]	3.677(5)	125.2(1)
O(12)[(4a)]-O(22)[(4a)]	3.728(5)	122.5(1)
Average	3.611	118.4

†Estimated standard errors in parentheses refer to the last digit. The equivalent positions (referred to Table 1) are designated as superscripts and are (1) = x, y, z; (2) = -y, x-y, z; (3) = y-x, -x, z; (4) = -x, -y, -z; (5) = y, y-x, -z; (6) = x-y, x, -z. The rhombohedral equipoints are: a = 2/3 1/3 1/3; b = 1/3 2/3 2/3.

*P–M, X shared edges. **M, X–M, X shared edges. For polyhedra a = apical, m = meridional.

Table 5 (continued)

M(10)

M(10)-O(14) [4a]	2.077(3)	
M(10)-O(9) [i]	2.135(3)	
M(10)-O(16) [5a]	2.153(3)	
M(10)-O(18) [4a]	2.232(3)	
M(10)-O(19) [4a]	2.312(3)	
M(10)-O(13) [5a]	2.613(4)	
Average (inner five)	2.182	

O(13) [5a] -O(16) [5a]	2.445(5)*	60.8(1)
a O(18) [4a] -O(19) [4a]	2.452(5)*	65.3(1)
O(9) [1] -O(13) [5a]	2.910(5)	74.8(1)
a O(14) [4a] -O(16) [5a]	2.983(5)	89.7(1)
a O(9) [1] -O(18) [4a]	3.003(4)**	86.9(1)
m O(9) [1] -O(19) [4a]	3.120(4)**	89.0(1)
a O(9) [1] -O(14) [4a]	3.213(5)	99.4(1)
a O(14) [4a] -O(19) [4a]	3.264(5)	96.0(1)
a O(16) [5a] -O(18) [4a]	3.334(5)	99.0(1)
O(13) [5a] -O(14) [4a]	3.487(5)	95.4(1)
O(13) [5a] -O(18) [4a]	>3.75 Å	104.3(1)
m O(16) [5a] -O(19) [4a]	>3.75 Å	133.6(1)
m O(9) [1] -O(16) [5a]	>3.75 Å	135.4(1)
Average apical	3.042	89.4
Average meridional	>3.540	119.3

Axial angle: O(14) [4a] -O(18) [4a] = 160.3(1)

M(11)

M(11)-O(11) [4a]	2.053(3)	
M(11)-O(13) [1]	2.079(3)	
M(11)-O(15) [3]	2.089(3)	
M(11)-O(10) [6a]	2.147(3)	
M(11)-O(21) [4a]	2.385(4)	
Average	2.151	

Apical edges

O(10) [6a] -O(13) [1]	2.785(5)	82.4(1)
O(11) [4a] -O(21) [4a]	2.904(5)	81.4(1)
O(10) [6a] -O(21) [4a]	2.970(4)**	75.3(1)
O(13) [1] -O(15) [3]	3.221(5)	101.2(1)
O(15) [3] -O(21) [4a]	3.305(5)	95.0(1)
O(11) [4a] -O(13) [1]	3.321(5)	107.0(1)
Average	3.084	90.4

Meridional edges

O(11) [4a] -O(15) [3]	3.472(5)	113.9(1)
O(10) [6a] -O(15) [3]	3.564(5)	114.6(1)
O(10) [6a] -O(11) [4a]	>3.75 Å	127.4(1)
Average	>3.595	118.6

Axial angle: O(13) [1] -O(21) [4a] = 156.5(1)

Ca

Ca-O(23) [3b]	2.366(3)
Ca-O(1) [5]	2.519(3)
Ca-O(1) [1]	2.570(3)
Ca-O(3) [1]	2.576(3)
Ca-O(8) [6]	2.679(4)
Ca-O(24) [4a]	2.680(5)
Ca-O(22) [4a]	2.722(4)
Ca-O(4) [5]	2.829(4)
Average	2.618

Ridgepole edges

O(3) [1] -O(22) [4a]	2.866(5)**	65.4(1)	55.3	2.501	O(1a)-O(1b)
O(4) [5] -O(23) [3b]	2.911(5)**	67.5(1)	77.2	2.811	O(3a)-O(3b)
Average	2.889	66.4	66.3	2.656	

Rafter edges

O(1) [1] -O(3) [1]	2.481(4)*	57.6(1)	51.0	2.452	O(3b)-O(6a)
O(1) [5] -O(4) [5]	2.487(4)*	55.1(1)	56.5	2.463	O(3a)-O(6b)
O(22) [4a] -O(24) [4a]	2.491(5)*	54.9(1)	61.4	2.685	O(3a)-O(6a)
O(1) [5] -O(22) [4a]	2.870(4)**	66.3(1)	56.2	2.731	O(3b)-O(6b)
O(3) [1] -O(8) [6]	2.926(5)**	67.7(1)	67.2	2.887	O(1b)-O(6b)
O(1) [1] -O(23) [3b]	3.009(5)	105.1(1)	75.4	3.055	O(1a)-O(6a)
O(4) [5] -O(8) [6]	3.168(5)	70.2(1)	86.4	3.487	O(1a)-O(6a)
O(23) [3b] -O(24) [4a]	>3.75 Å	97.0(1)	89.4	3.791	O(1b)-O(6b)
Average	>2.898	71.7	67.9	2.944	

Tie beam edges

O(1) [1] -O(8) [6]	3.095(5)	72.2(1)	79.6	3.136	O(6a)-O(6b)
O(1) [5] -O(24) [4a]	3.420(5)	82.2(1)	80.2	3.221	O(6a)-O(6b)
O(1) [5] -O(8) [6]	>3.75 Å	101.9(1)	97.6	3.660	O(6a)-O(6a)
O(1) [1] -O(24) [4a]	>3.75 Å	103.8(1)	100.0	3.854	O(6b)-O(6b)
Average	>3.504	90.0	89.4	3.468	

X(2) in Wyllieite

2.380	X(2)-O(6a)
2.415	X(2)-O(6b)
2.485	X(2)-O(6a)
2.608	X(2)-O(1a)
2.614	X(2)-O(6b)
2.753	X(2)-O(3a)
2.772	X(2)-O(1b)
3.108	X(2)-O(3b)
2.642	

is the longest X–O distance for that coordination polyhedrom and is also listed in the bond distance tables. This is followed by the next larger distance found in fillowite's structure but not used in calculations or entered in tables which follow. If that distance involves an anion (X–O), it is italicized since it could potentially be a coordinating anion to X. However, there exists a substantial gap between this distance and that in the preceding column, the smallest difference being for Na(2)–O where [Na(2)–O(16)]–

Table 5 (continued)

Na(1)			P(1)			P(4)		
3 Na(1)–O(14)[1]	2.448(4)		P(1)–O(4)	1.533(3)		P(4)–O(13)	1.520(3)	
3 Na(1)–O(10)[4a]	2.449(4)		P(1)–O(1)	1.535(3)		P(4)–O(14)	1.523(4)	
Average	2.449		P(1)–O(3)	1.540(3)		P(4)–O(15)	1.545(3)	
			P(1)–O(2)	1.552(3)		P(4)–O(16)	1.555(3)	
			Average	1.540		Average	1.536	
3 O(10)[4a]–O(10)[5a]	3.057(5)**	77.3(1)						
3 O(10)[4a]–O(14)[1]	3.367(5)	86.9(1)	O(2)–O(4)	2.454(5)*	105.4(2)	O(13)–O(16)	2.445(5)*	105.3(2)
3 O(14)[1]–O(14)[2]	3.455(6)**	89.8(1)	O(1)–O(3)	2.481(4)*	107.6(2)	O(13)–O(14)	2.496(5)	110.2(2)
3 O(10)[6a]–O(14)[1]	>3.75 Å	108.1(1)	O(1)–O(3)	2.487(4)*	108.3(2)	O(13)–O(15)	2.498(5)	109.2(2)
Average	>3.407	90.5	O(2)–O(3)	2.495(5)	107.6(2)	O(14)–O(16)	2.505(5)	108.9(2)
			O(1)–O(2)	2.578(4)	113.2(2)	O(15)–O(16)	2.536(5)	109.8(2)
			O(3)–O(4)	2.590(5)	115.0(2)	O(14)–O(15)	2.560(5)	113.2(2)
Na(2)			Average	2.514	109.5	Average	2.507	109.4
3 Na(2)–O(7)[4a]	2.563(4)							
3 Na(2)–O(14)[1]	2.683(4)							
Average	2.623		P(2)			P(5)		
			P(2)–O(6)	1.527(3)		P(5)–O(17)	1.506(3)	
3 O(7)[4a]–O(7)[5a]	2.826(6)**	66.9(1)	P(2)–O(6)	1.532(3)		P(5)–O(20)	1.546(3)	
3 O(14)[1]–O(14)[2]	3.455(6)**	80.2(1)	P(2)–O(8)	1.537(3)		P(5)–O(19)	1.548(3)	
3 O(7)[4a]–O(14)[1]	>3.75 Å	99.5(1)	P(2)–O(7)	1.551(3)		P(5)–O(18)	1.563(3)	
3 O(7)[6a]–O(14)[1]	>3.75 Å	114.5(1)	Average	1.537		Average	1.541	
Average	>3.445	90.3						
			O(6)–O(7)	2.444(5)	105.1(2)	O(18)–O(19)	2.452(5)*	104.0(2)
Na(3)			O(5)–O(8)	2.479(4)	107.7(2)	O(17)–O(19)	2.503(5)*	110.1(2)
			O(5)–O(7)	2.507(5)	108.8(2)	O(18)–O(20)	2.504(4)	107.3(2)
Na(3)–O(9)[4a]	2.357(4)		O(5)–O(6)	2.533(5)	111.8(2)	O(17)–O(18)	2.521(5)*	110.4(2)
Na(3)–O(18)[1]	2.474(4)		O(7)–O(8)	2.545(5)	111.0(2)	O(17)–O(20)	2.549(4)	113.3(2)
Na(3)–O(17)[5a]	2.488(4)		O(6)–O(8)	2.546(5)	112.4(2)	O(19)–O(20)	2.554(4)	111.3(2)
Na(3)–O(19)[5a]	2.513(4)		Average	2.509	109.5	Average	2.514	109.4
Na(3)–O(9)[2]	2.575(4)							
Na(3)–O(11)[2]	2.740(4)		P(3)			P(6)		
Na(3)–O(17)[1]	2.835(5)							
Average	2.563		P(3)–O(9)	1.530(3)		P(6)–O(24)	1.519(4)	
			P(3)–O(10)	1.550(3)		P(6)–O(23)	1.530(3)	
O(17)[5a]–O(19)[5a]	2.503(5)*	60.1(1)	P(3)–O(12)	1.551(3)		P(6)–O(21)	1.536(3)	
O(9)[2]–O(11)[2]	2.517(5)*	56.4(1)	P(3)–O(11)	1.554(3)		P(6)–O(22)	1.584(3)	
O(17)[1]–O(18)[1]	2.521(5)*	56.2(1)	Average	1.546		Average	1.542	
O(11)[2]–O(18)[1]	2.800(4)**	64.7(1)						
O(9)[4a]–O(18)[1]	3.003(4)**	76.8(1)	O(11)–O(12)	2.468(4)*	105.3(2)	O(21)–O(22)	2.476(5)	105.0(2)
O(17)[1]–O(17)[5a]	3.033(5)**	69.1(1)	O(10)–O(11)	2.511(5)	108.0(2)	O(22)–O(24)	2.491(5)*	106.7(2)
O(9)[2]–O(19)[5a]	3.120(4)**	75.5(1)	O(9)–O(11)	2.517(5)*	109.4(2)	O(22)–O(23)	2.505(5)	107.1(2)
O(9)[4a]–O(17)[1]	3.330(5)**	79.2(1)	O(9)–O(12)	2.535(4)	110.8(2)	O(21)–O(23)	2.511(5)	110.0(2)
O(9)[2]–O(17)[5a]	3.330(5)**	82.2(1)	O(9)–O(10)	2.549(4)	111.7(2)	O(23)–O(24)	2.535(5)	112.5(2)
O(9)[4a]–O(19)[5a]	>3.75 Å	106.0(1)	O(10)–O(12)	2.563(4)	111.5(2)	O(21)–O(24)	2.574(5)	114.9(2)
O(11)[2]–O(19)[5a]	>3.75 Å	112.5(1)	Average	2.524	109.4	Average	2.515	109.4
O(9)[4a]–O(11)[2]	>3.75 Å	106.4(1)						
O(9)[4a]–O(17)[5a]	>3.75 Å	116.1(1)						
O(17)[5a]–O(18)[1]	>3.75 Å	120.4(1)						
Average	>3.208	84.4						

[Na(2)–O14] = 0.16Å. It is admitted that the cutoff for X–O bond distances is arbitrary, guided only by suggested averages in Shannon and Prewitt (1969). For the Na(3) polyhedron for example, there exist five distances between 2.36–2.58Å defining a distorted trigonal bipyramid but two additional distances between 2.74 and 2.84Å were included result-

ing in Na(3)O₇ or polyhedron No. 13 of order 7 with maximal point symmetry $C_s(m)$ listed by Britton and Dunitz (1973). This tendency toward coordination greater than six emphasizes the problem with glaserite-derived structures as discussed in some detail and with abundant illustrations by Moore (1981).

The structure can be described in two ways, one

Table 6. Fillowite: some characteristics of the nonequivalent cations†

Atom	ERN	C.N.	$\langle X-O \rangle$	Scattering Curve	Largest X–O in Table 5		Next Larger in Fillowite	
M(1)	3	6	2.254 Å	0.62(3) Mn^{2+} + 0.38 Ca^{2+}	M(1)-O(24)	2.25 Å	M(1)-P(6)	3.55 Å
M(2)	3	6	2.204	1.00 Mn^{2+}	M(2)-O(17)	2.20	M(2)-P(5)	3.64
M(3)	6	6	2.175	1.00 Fe^{2+}	M(3)-O(10)	2.33	M(3)-Na(1)	3.22
M(4)	6	6	2.133	1.00 Fe^{2+}	M(4)-O(2)	2.16	M(4)-P(2)	3.20
M(5)	6	6	2.198	1.00 Mn^{2+}	M(5)-O(2)	2.34	M(5)-M(7)	3.19
M(6)	18	5	2.145	1.00 Mn^{2+}	M(6)-O(1)	2.17	*M(6)-O(6)*	*2.70*
M(7)	18	6	2.235	1.00 Mn^{2+}	M(7)-O(3)	2.45	*M(7)-O(2)*	*2.82*
M(8)	18	6	2.198	0.67 Fe^{2+} + 0.33 Mn^{2+}	M(8)-O(5)	2.28	M(8)-P(4)	3.37
M(9)	18	5	2.141	1.00 Mn^{2+}	M(9)-O(11)	2.29	M(9)-P(3)	2.81
M(10)	18	5-6	2.182	1.00 Mn^{2+}	M(10)-O(13)	2.61	M(10)-P(5)	2.85
M(11)	18	5	2.151	1.00 Mn^{2+}	M(11)-O(21)	2.39	*M(11)-O(10)*	*2.98*
Na(1)	6	6	2.449	0.91(2) Na^{1+} + 0.09 Ca^{2+}	Na(1)-O(10)	2.45	*Na(1)-O(13)*	*3.14*
Na(2)	6	6	2.623	0.90(2) Na^{1+} + 0.10 Ca^{2+}	Na(2)-O(14)	2.68	*Na(2)-O(16)*	*2.84*
Na(3)	18	7	2.563	1.00 Na^{1+}	Na(3)-O(17)	2.84	Na(3)-P(5)	3.02
Ca	18	8	2.618	0.65(1) Ca^{2+} + 0.35 Na^{1+}	Ca-O(4)	2.83	Ca-P(1)	3.16
P(1)	18	4	1.540	1.00 P^{5+}				
P(2)	18	4	1.537	1.00 P^{5+}				
P(3)	18	4	1.546	1.00 P^{5+}				
P(4)	18	4	1.536	1.00 P^{5+}				
P(5)	18	4	1.541	1.00 P^{5+}				
P(6)	18	4	1.542	1.00 P^{5+}				

†Headed as atomic label, equipoint rank number (ERN), coordination number (C.N.), mean X–O distance, scattering curves used in refinement, largest X–O distance in Table 4, and next larger distance in the structure.

treating the arrangement as a packing of rods, diagrams (Fig. 1a–1c) of which appeared in Moore (1981). Figure 1a shows the packing of the rods as a *plan*, as viewed down the [001] direction. Three distinct rods occur in the structure, illustrated by Roman numerals I, II, and III. Rods I and II consist of large cations only in the sequence $\cdots$ X–X–X–X $\cdots$. These rods occur at the centers of a hexagonal tessellation $\{6^3\}$. At the nodes of $\{6^3\}$, rod III occurs with sequence $\cdots$ T–X–T–X–T–□(1)–T–X–T–X–T–□(2) $\cdots$ where T is a tetrahedrally coordinated cation (P^{5+}), X a larger cation and □ an ordered vacancy. As the ratio of centers to nodes in $\{6^3\}$ is 1:2, the solution is evidently I + II:4III or 12X + 12X:4(4X + 2□ + 6T) which gives a ratio $\square_8 X_{40} T_{24}$ or X:T = 5:3. In Figure 1a the $\{6^3\}$ net, drawn directly on the projected structure with enveloping circles encompassing the cations in a rod, is remarkably regular suggesting that fillowite's structure can be best conceived as a hexagonal rod packing. This property makes the rod description of so extraordinarily complex a structure appealing. In Figure 1b, rod I is shown as a Pen-

Table 7. Fillowite chemical analyses and interpretation†

	1	2	3	4	5	6	7
Li_2O	0.06	0.07	--	--	0.11	--	0.60
Na_2O	5.74	5.44	5.93	5.96	5.65	4.8	5.94
K_2O	--	--	--	--	0.20	--	0.15
CaO	4.08	3.63	3.58	5.39	4.80	6.2	4.86
MgO	--	--	--	--	tr	12.9	10.12
FeO	9.33	9.69	--	--	19.41	26.8	19.18
MnO	39.42	39.58	49.76	47.72	26.50	5.1	12.39
Al_2O_3	--	--	--	--	tr	--	1.44
P_2O_5	39.10	39.68	40.73	40.93	40.70	44.8	42.84
H_2O	1.66	1.58	--	--	0.56	--	0.55
Rem.	0.88	1.02	--	--	2.35	--	--
Total	100.27	100.69	100.00	100.00	100.28	100.6	98.07

[1]Brush and Dana (1879). Remainder is quartz.

[2]Brush and Dana (1890). Remainder is quartz.

[3]Computed analysis for $Na_3CaMn_{11}^{2+}(PO_4)_9$ with calculated density $\rho = 3.550$ g cm^{-3}. Brush and Dana (1879) report specific gravity 3.43.

[4]Computed for $Na_2CaMn_7^{2+}(PO_4)_6$ with calculated density $\rho = 3.533$ g cm^{-}

[5]Fillowite with much iron. Kabira, Uganda. Von Knorring (1963). Remainder includes Fe_2O_3 1.98 and SiO_2 0.37.

[6]Johnsomervilleite from Livingstone (1980). Average of three probe analyses.

[7]Johnsomervilleite (metamict) from Sapucaia pegmatite, Brazil. Probe analysis by D. McKeown, atomic absorption analysis by A. Davis and water determination (Penfield tube) by P. B. Moore.
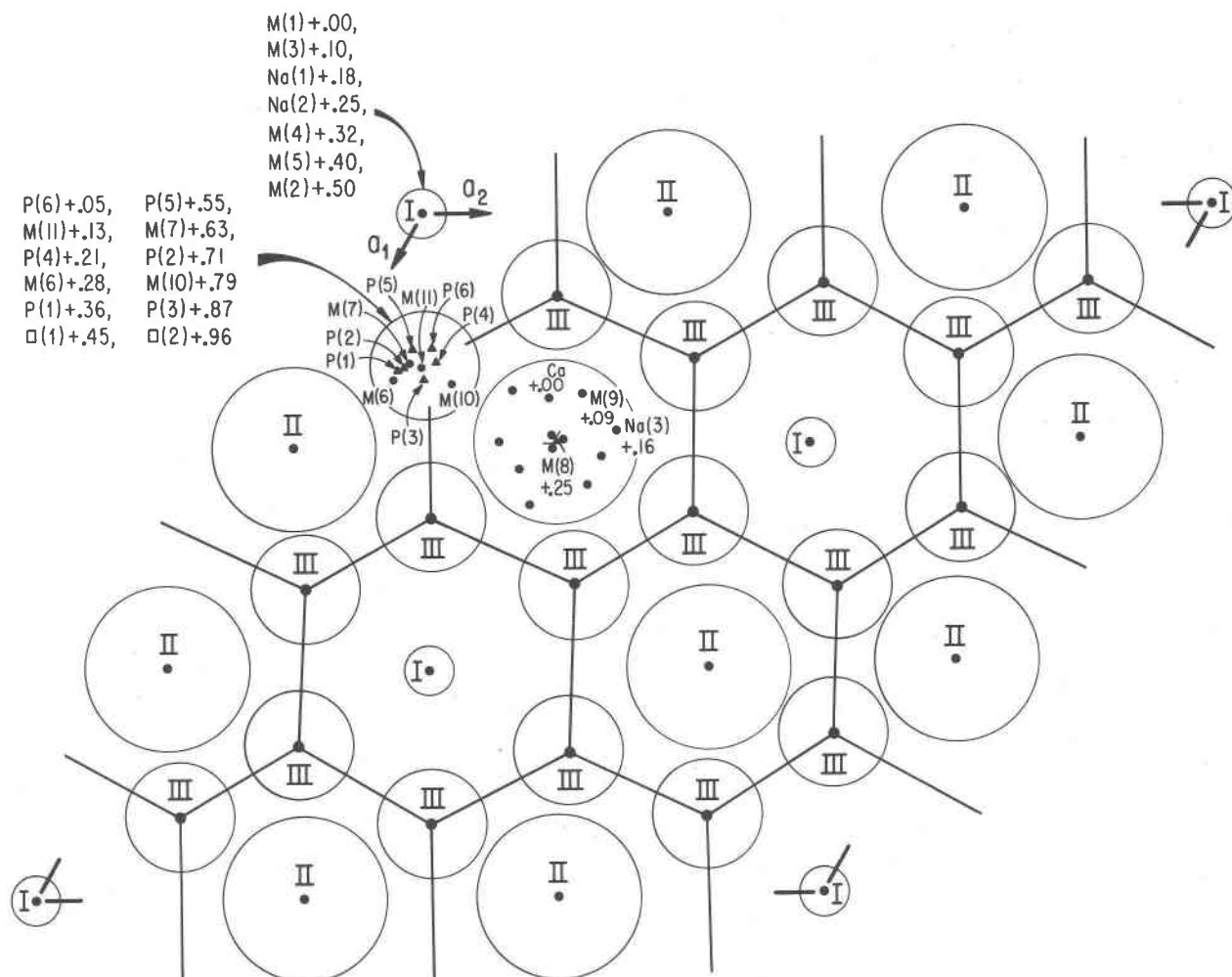
Fig. 1a. Plan of the cations in fillowite projected down [001]. Rod I at $x,y = 0, 0$, etc., and rod II at the 3_1-screw axis 1/3, 1/3, etc., are centered in the hexagonal net [6^3]. Rod III is at the nodes of the net at 2/9, 1/9, etc., and includes all the P atoms. Atoms and heights in z in the asymmetric unit are labelled. Circles are the envelopes about the cation positions.

field projection (Penfield, 1905; Moore, 1981), a convenient vehicle for displaying such a structure with insular corner-linked octahedra followed by five face-sharing octahedra. If we fill the slots between the face-sharing octahedral units with trigonal prisms Δ the sequence is –M–Δ–M–M–M–M–M–Δ–M–Δ–M–M–M–M–M–Δ–, or 16 polyhedra in the c-repeat, distinct from 12 if such Δ were ignored. Twelve layers or twelve cations in the rod repeat appears to be the case for fillowite, and $c/12 = 43.51/12 = 3.63$Å is the appropriate interlayer repeat in such glaserite derived structures. Figure 1c shows the sequence along rod II as a Penfield projection and these have been discussed earlier (Moore, 1981). Note that in this map only the six inner oxygens are featured about Ca (bonds Ca–O 2.37–2.68Å) *not* the remaining two Ca–O(22) 2.72 and Ca–O(4) 2.83Å distances. The same

applies to Na(3)O₅, where the two longer distances Na(3)–O(11) 2.74 and Na(3)–O(17) 2.84Å are not shown in the stippled polyhedron. Rod II weaves about the 3_1-axis in the c-repeat sequence ··· Ca–M(9)–Na(3)–M(8)–Ca–M(9)–Na(3)–M(8)–Ca–M(9)–Na(3)–M(8) ····.

The rod III sequence is not featured as a Penfield projection. Its sequence, positioned at the nodes of the {6^3} net, is ··· P(6)–M(11)–P(4)–M(6)–P(1)–□(1)–P(5)–M(7)–P(2)–M(10)–P(3)–□(2) ····. All six nonequivalent (PO₄) tetrahedra occur in this rod. Note the alternating of P with M, or P with an intervening vacancy. These are the vacancies that were counted in the □₈X₄₀T₂₄ enumeration as discussed earlier.

The next sequence of figures shows fillowite's structure in more traditional projections down [001], where the structure is taken apart into layers or
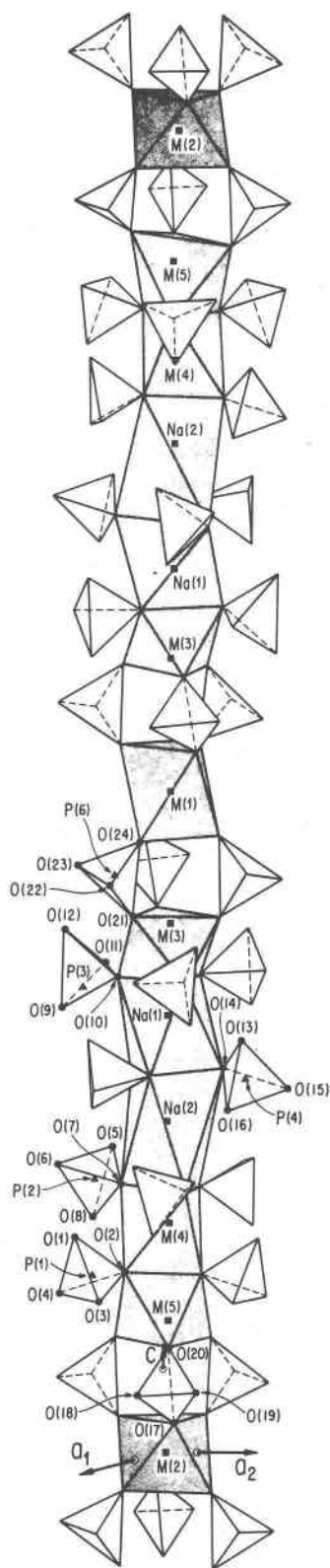
Fig. 1b. Penfield projection of rod I in fillowite, with circumjacent tetrahedra. The origin, shown as arrows, is 0 0 1/2.
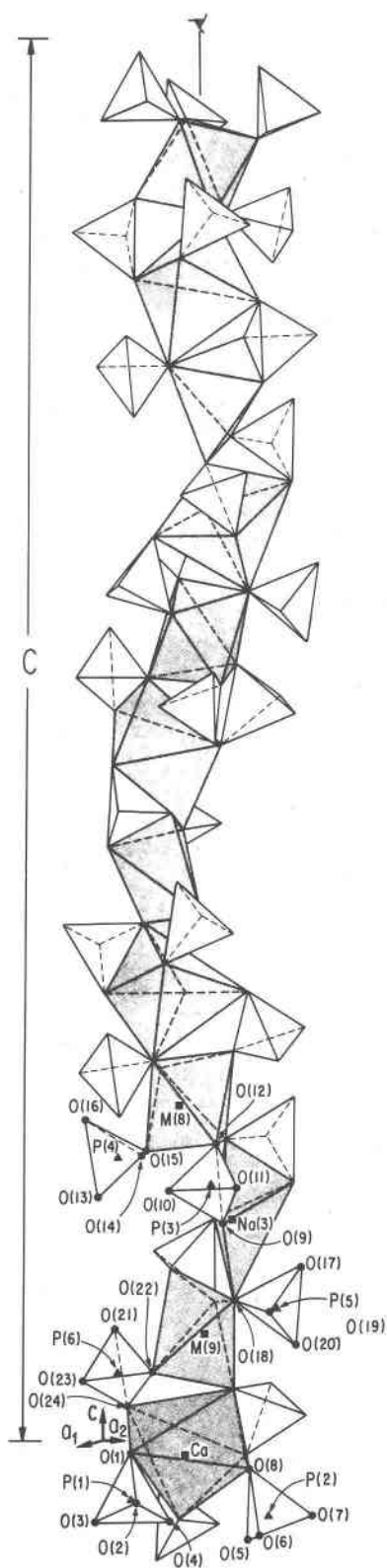
Fig. 1c. Penfield projection of rod II in fillowite with circumjacent tetrahedra. Note Ca and Na(3) are not complete since they are actually CaO_8 and $Na(3)O_7$. The polyhedra weave about the 3_1-axis.
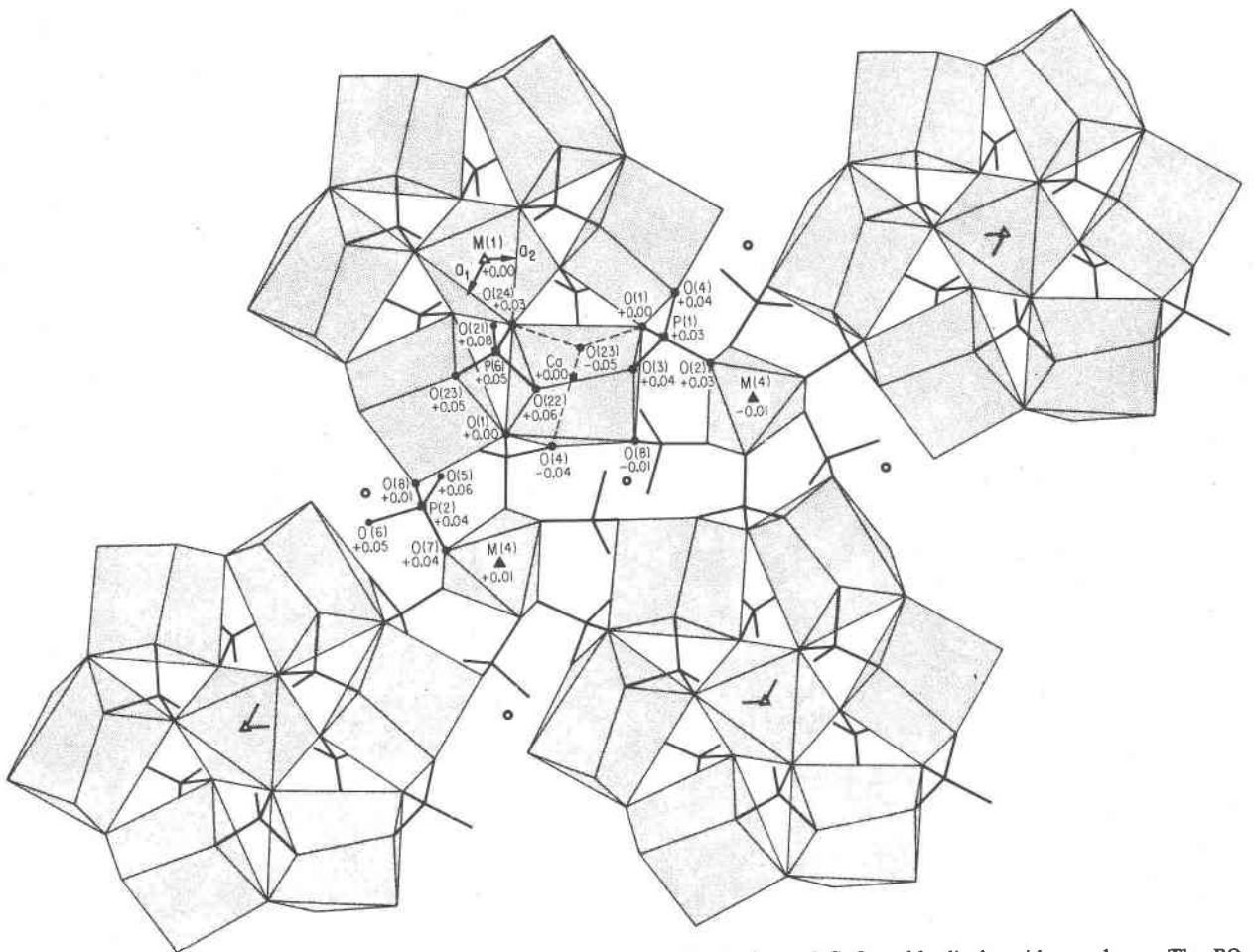
Fig. 2a. Conventional projection of the slab about $z = 0$ in fillowite. Octahedra and CaO_8 gable disphenoids are shown. The PO_4 tetrahedra are drawn as spokes. Atoms in the asymmetric unit with heights in z are labelled. Inversion centers are drawn as open circles and the 3-axes as solid triangles.
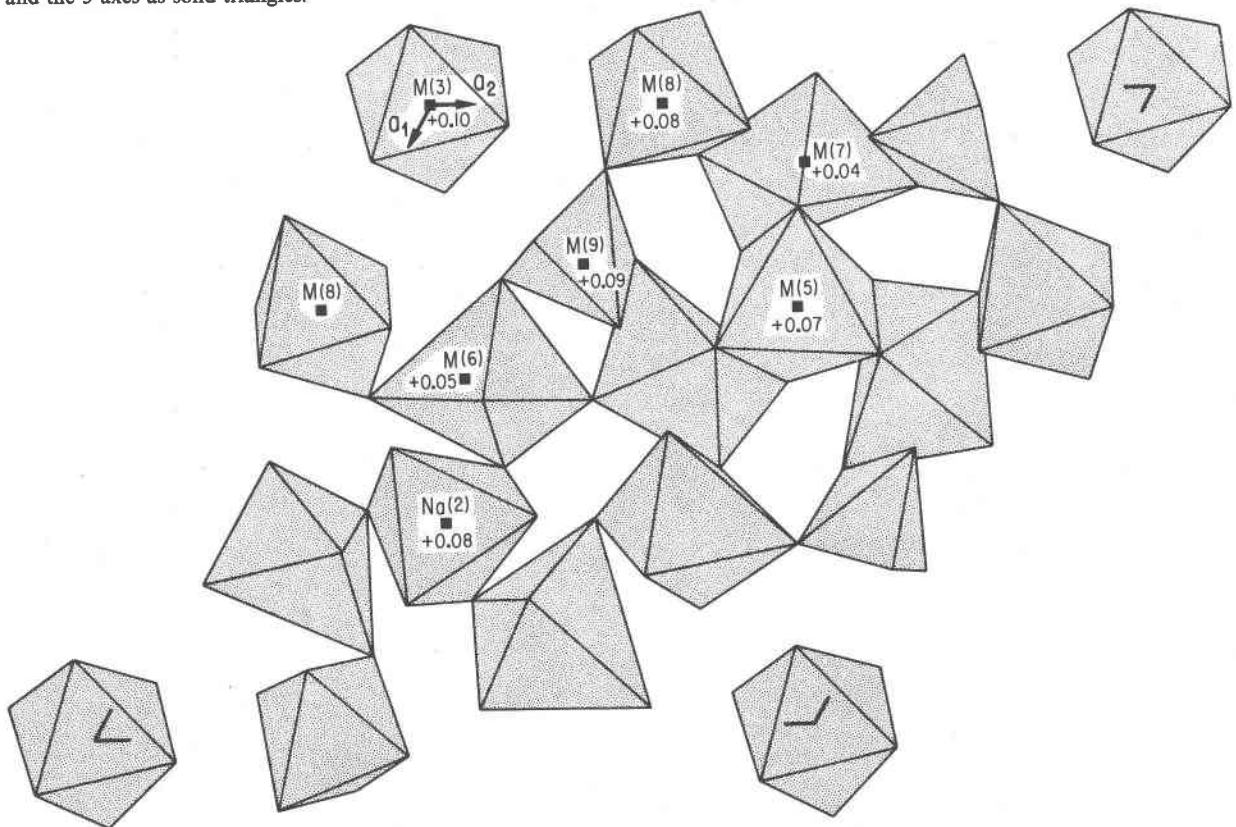
Fig. 2b. Conventional projection of the slab at $z = 1/12$ showing only the larger polyhedra. Atoms in the asymmetric unit with heights in z are labelled. M(3), M(5), M(7), M(8) and Na(2) are octahedra; M(6) and M(9) are five-coordinated.
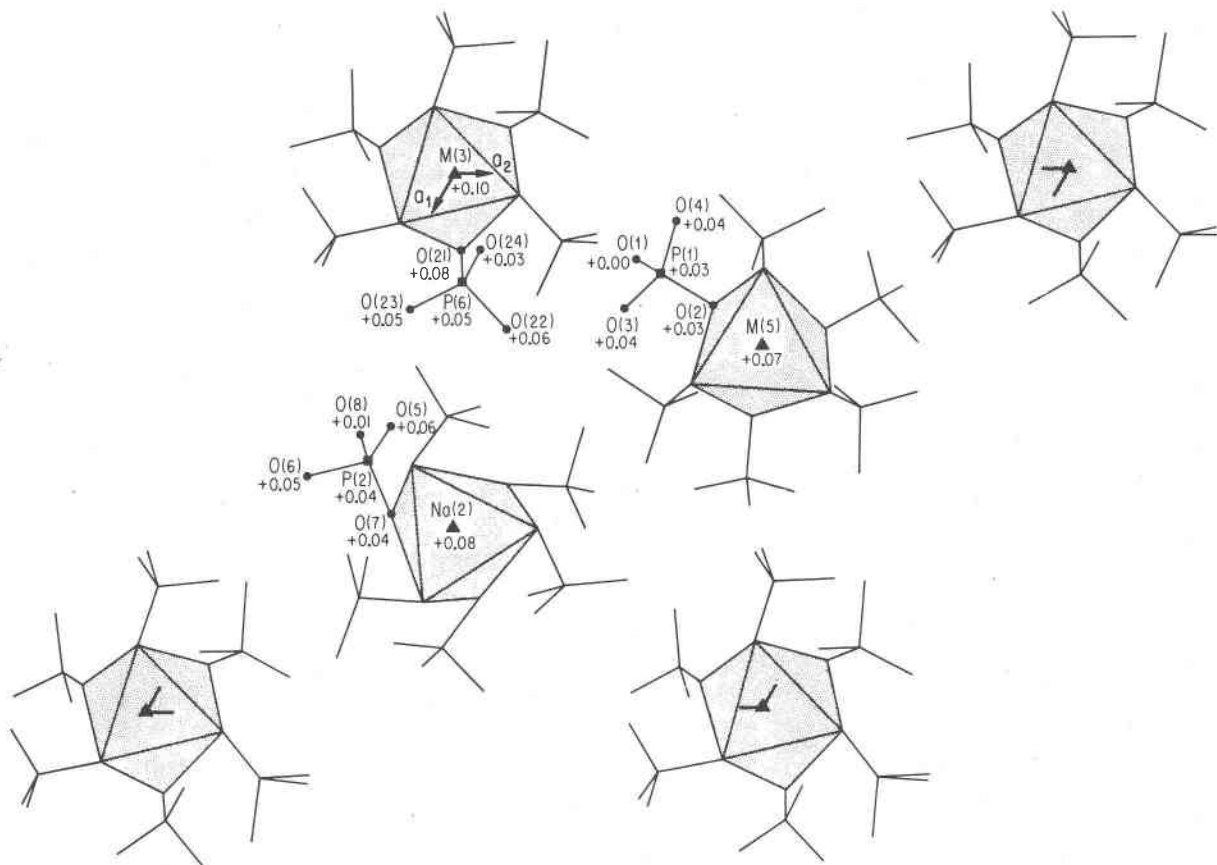
Fig. 2c. Spoke diagram of tetrahedra for 2b with octahedra at 3-fold rotors retained. Atoms in the asymmetric unit with heights in z are labelled.
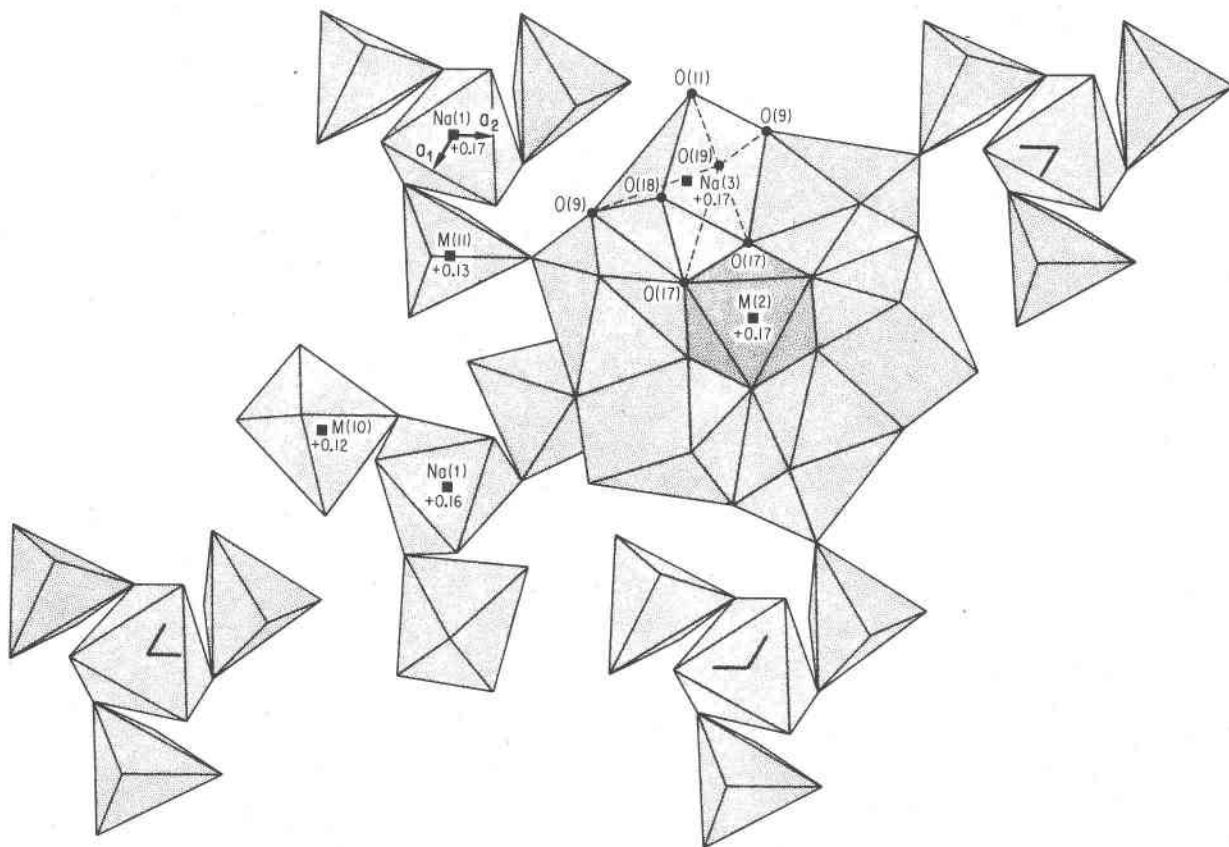
Fig. 2d. Conventional projection of the slab at $z = 2/12$ showing only the larger polyhedra. Atoms in the asymmetric unit with heights in z are labelled. M(2) and Na(1) are octahedra, M(10) is either a distorted octahedron or, like M(11), five coordinated.
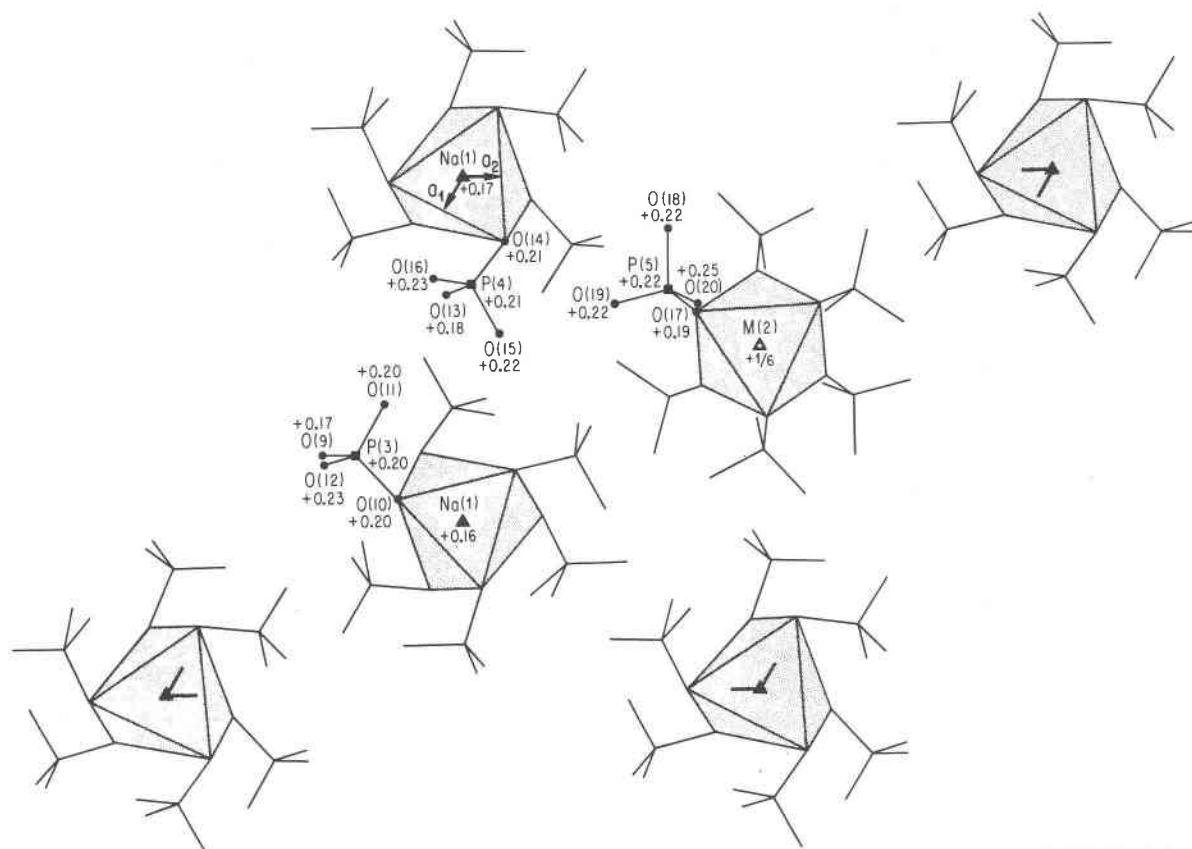
Fig. 2e. Spoke diagram of tetrahedra for 2d with octahedra at 3-fold rotors retained. Note inversion center at 1/3 2/3 1/6. Atoms in the asymmetric unit with heights in z are labelled.

sheets. As the c-repeat has the sequence 0/12, 1/12, 2/12, $\cdots$ 11/12 we need only represent the first three, because inversion centers occur at (0 0 0) and (1/3 2/3 1/6), etc., for $R\bar{3}$. Figure 2a that $\sim$0/12 is perhaps the most interesting. It shows $M(1)O_6$ and $M(4)O_6$ octahedra on 3-fold rotors with M(1) linked to form a pinwheel array of six CaO_8 *gable disphenoids*. This polyhedron has received considerable discussion (Moore, 1981). The PO_4 tetrahedra share corners and edges to form an interesting sheet. Bond distances and angles for all pertinent polyhedra appear in Table 5. The *gable disphenoid* in fillowite is compared directly with a similar polyhedron called X(2) in wyllieite (Moore and Molin-Case, 1974) and the distances and angles in both data sets compare well. The *gable disphenoid* was overlooked in the earlier study so most of these calculations are new. In fillowite, foreshortening of shared edges for the polyhedra are grouped toward the top of the list of edge distances in Table 5 as all distances were arranged according to increasing values. The distances involving shared edges reflect also the neighboring

polyhedral size, in particular the small PO_4 tetrahedron.

In Figures 2b and 2c the level at $z \sim 1/12$ is featured, the former showing only the larger cation coordination polyhedra, the latter the polyhedra at (0 0 $\sim$ 1/12), (2/3 1/3 $\sim$ 1/12), (1/3 2/3 $\sim$ 1/12) with the linking tetrahedra drawn as spokes. It was necessary to separate this level into two drawings in order to avoid hopeless clutter. The coordination numbers of the larger cations are [6]M(3), [6]M(5), [5]M(6), [6]M(7), [6]M(8), [5]M(9) and [6]Na(2). The six-coordinated cations are associated with distorted octahedra. For the five-coordinated polyhedra, M(6) was drawn as an octahedron (O(1) is below the plane of the shading) but M(6)–O(6) 2.699Å is considered too long even though it is drawn in. The O(6) is the corner-link between M(6) and M(7). In following discussions, this bond will be ignored, and M(6) is considered a distorted square pyramid. M(9) appears to be closer to a trigonal bipyramid and the bond distances are arrayed accordingly in Table 5, with six apical edges, three meridional edges and an axial

Table 8. Fillowite: electrostatic valence balance of cations and anions†

Anions	M(1)	M(2)	M(3)	M(4)	M(5)	M(6)	M(7)	M(8)	M(9)	M(10)	M(11)	Ca	Na(1)	Na(2)	Na(3)	P(1)	P(2)	P(3)	P(4)	P(5)	P(6)	Δp_0
O(1)						1						2				1						+0.15
						+.029						−.099				−.005						
												−.048										
O(2)				1	1		1										1					+0.25
				+.030	+.139		+.170										+.012					
O(3)						1		1			1					1						+0.23
						+.214		−.045			−.042					+.000						
O(4)						1	1				1					1						+0.16
						+.115	−.068				+.061					−.007						
O(5)						1		1												1		−0.02
						+.009		+.081												−.005		
O(6)							1													1		−0.42
							−.191													−.010		
O(7)				1		1								1		1						+0.15
				−.030		+.002								−.060		+.014						
O(8)							1				1						1					−0.17
							−.192				+.061						+.000					
O(9)									1						2		1					−0.06
									−.047						−.206							
															+.012		−.016					
O(10)			1							1				1					1			+0.15
			+.158							−.004				+.000					+.004			
O(11)									1		1				1		1					+0.19
									+.148		−.098				+.177		+.008					
O(12)								1	1										1			−0.02
								+.021	+.039										+.005			
O(13)								1	1											1		+0.05
								+.431	−.072											−.016		
O(14)										1			1	1						1		−0.02
										−.105			−.001	+.060						−.013		
O(15)								1			1									1		−0.02
								−.044			−.062									+.009		
O(16)						1			1											1		+0.05
						−.003			−.029											+.019		
O(17)		1													2					1		−0.13
		+.000													−.075					−.035		
															+.272							
O(18)							1	1							1					1		+0.19
							−.071	+.050							−.089					+.022		
O(19)							1		1						1					1		+0.13
							−.006		+.130						−.050					+.007		
O(20)				1		1														1		−0.08
				−.140		−.116														+.005		
O(21)		1								1											1	−0.02
		−.168								+.234											−.008	
O(22)				1			1			1											1	+0.30
				−.035			−.070			+.104											+.042	
O(23)							1			1											1	−0.17
							+.019			−.252											−.012	
O(24)	1									1											1	−0.17
	+.000									+.062											−.023	

†A bond length deviation refers to the polyhedral average subtracted from the individual bond distance. The Δp_0 = deviations of electrostatic bond strength sum from neutrality ($p_0 = 2.00$ e.s.u.). Bond length deviations which conform to Δp_0 are italicized.

Table 9. Fillowite: calculated and observed powder patterns†

I(calc)	d(calc)	hkl	I(obs)	d(obs)
7	14.503	003		
30	11.306	012	35	11.438
17	8.403	104	20	8.492
5	7.251	006	5	7.352
3	6.331	202	5	6.365
10	5.653	024	10	5.690
17	5.260	116	10	5.288
		?	5	5.158
11	4.545	214	10	4.565
6	4.337	125	5	4.367
7	4.221	303	5	4.252
38	3.769	306	40	3.789
14	3.694	223	5	3.716
18	3.626	00.12	65	3.640
40	3.619	312		
12	3.478	134	10	3.492
9	3.380	226	10	3.397
5	3.283	21.10	5	3.293
4	3.259	309	10	3.234
7	3.165	404	5	3.172
20	3.025	01.14	10	3.029
45	3.007	232	70	3.017
7	2.997	229		
5	2.924	324	10	2.935
7	2.888	410	10	2.896
5	2.867	235	5	2.873
21	2.832	413	10	2.843
31	2.813	20.14		
12	2.805	13.10	100	2.814
100	2.801	30.12		
5	2.690	31.11	10	2.692
8	2.683	416		
6	2.640	12.14	10	2.647
59	2.547	330	60	2.552
7	2.497	241	5	2.500
23	2.403	336	10	2.408
6	2.389	21.16	5	2.390
5	2.372	31.14	10	2.367
5	2.363	152		
			5	2.25
8	2.173	431	20	2.16
7	2.165	342		
8	2.084	33.12	5	2.10
9	2.043	22.18	5	2.04
3	2.015	50.14	5	2.01

†Calculations based on FeKα radiation and parameters in Table 1. The observed data are from Fisher (1965). His observed intensities are x10.

angle given. The bridging PO_4 tetrahedra are labelled according to their coordinates in Table 1.

In Figures 2d and 2e are the coordination polyhedra at $z \sim 2/12$. In Figure 2d, there are the [6]M(2), [6]M(10), [5]M(11), [6]Na(1) and [7]Na(3) polyhedra. M(2) and Na(1) reside in distorted octahedra. The coordination of M(10), like that of M(6) as noted, is problematical. The M(10)–O(13) 2.613Å bond is perhaps too long as the average for the inner five bonds is 2.182Å. Therefore in Table 5, the M(10)–O bonds were listed both as an octahedral model and as a trigonal bipyramidal model. The O(13) site is the one immediately below the M(10) designation in Figure

2d. M(11) appears to be a distorted trigonal bipyramid. The geometry of the Na(3)O_7 polyhedron is difficult to define. Initially, [5]Na(3) was selected as a distorted trigonal bipyramid but with two additional bonds as mentioned before it becomes Na(3)O_7. Beyond this is a Na(3)–P(5) distance (Table 6) so an upper limit of seven coordination appears reasonable. The polyhedron shares edges with equivalent polyhedra and edges with the central M(2)O_6 octahedron.

Bond distances and angles

In such an elephantine structure as fillowite, bond distance and angle tabulations are long and tedious as borne out by Table 5. The distances were deliberately listed as increasing values for each polyhedron and when the polyhedron possessed more than one orbit (equivalence class), the edges were partitioned into the appropriate classes. For example, in the trigonal bipyramid, apical edges and meridional edges constitute the two categories. For the *gable disphenoid,* three orbits exist, defining the ridge pole edges, rafter edges and tie beam edges, terms previously used by Moore (1981). For a more complex polyhedron of low symmetry (such as Na(3)O_7), no distinction was made.

Several interesting properties can be noted in Table 5. In rod I, the sequences of face-sharing octahedra ⋯ M(3)–Na(1)–Na(2)–M(4)–M(5) ⋯ are expected to show considerable distortion at the terminal M(3) and M(5) octahedra due to the cation-cation repulsion effects. We would expect the terminal O_a–M–O'_a angle to widen and the opposing O_b–M–O'_b to foreshorten. This a rather pronounced effect in fillowite, with O(20)–M(5)–O(20)′ 110.2° and O(21)–M(3)–O(21)′ 109.1° for the terminal angles. The opposing angles toward the face-sharing direction, are O(2)–M(5)–O(2)′ 70.9° and O(10)–M(3)–O(10)′ 81.9°, the more pronounced effect being associated with M(5) which shares a face with another divalent octahedron, M(4). The M(3) terminal octahedron shares its face with Na(1) and the effect is therefore less pronounced.

Another important effect is the foreshortening of shared polyhedral edges, which tend to occur at the top of the entries in Table 5. Most noticeable perhaps is Na(3): of fourteen edges listed, the first nine all involve shared edges and within these, the first three correspond to edges shared with tetrahedra.

Another interesting feature is that meridional edges tend not to be shared among the trigonal bipyramids. Of the seven shared edges listed, only

one—O(9)–O(19)—is a meridional edge. This is also noticed for the CaO_8 polyhedron: both ridge pole edges, five of the eight rafter edges and none of the four tie beam edges are shared. The tie beam edges are much like the meridional edges in the trigonal bipyramid.

Electrostatic valence balance calculations of cations about anions appear in Table 8. Of the 84 distinct entries, 49 conform in their distance deviations with the net electrostatic deviations from neutrality. The remaining 35 contradictions are largely compensated by trends in the opposite direction. The most pronounced deviation is $\Delta p_0 = -0.42$ for O(6). Here the distance contractions from the polyhedral average are particularly noticeable.

When a structure is known and reasonably well-refined it is advantageous to calculate a powder diffraction pattern directly from the pertinent structure cell parameters. Such a calculation appears in Table 9, and is compared with the results of Fisher (1965) for fillowite from the type locality. The agreement is excellent, the only obvious advantage to the calculated data being found in the correct choice of Miller indices.

Acknowledgments

References

Britton, D. and Dunitz, J. D. (1973) A complete catalogue of polyhedra with eight or fewer vertices. Acta Crystallographica, A29, 362–371.

Brush, G. J. and Dana, E. S. (1878) On a new and remarkable mineral locality in Fairfield County, Connecticut; with description of several new species occurring there. American Journal of Science, 16, 33–46.

Brush, G. J. and Dana, E. S. (1890) On the mineral locality at Branchville, Connecticut. With analyses of several manganesian phosphates by H. L. Wells. American Journal of Science, 39, 201–216.

Cromer, D. T. and Liberman, D. (1970) Relativistic calculation of anomalous scattering factors for X-rays; Los Alamos Scientific Laboratory, University of California Report LA-4403, University of California-34.

Cromer, D. T. and Mann, J. B. (1968) X-ray scattering factors computed from numerical Hartree-Fock wave-functions. Acta Crystallographica, A24, 321–324.

Fisher, D. J. (1965) Dickinsonite, fillowite and alluaudites. American Mineralogist, 50, 1647–1669.

Livingstone, A. (1980) Johnsomervilleite, a new transition-metal phosphate mineral from the Loch Quioch area, Scotland. Mineralogical Magazine, 43, 833–836.

Moore, P. B. (1981) Complex crystal structures related to glaserite, $K_3Na(SO_4)_2$: evidence for very dense packing among oxysalts. Bulletin de la Société Française de Minéralogie et de Cristallographie, in the press.

Moore, P. B. and Molin-Case, J. A. (1974) Contribution to pegmatite giant crystal paragenesis: II. The crystal chemistry of wyllieite, $Na_2Fe_2Al(PO_4)_3$, a primary phase. American Mineralogist, 59, 280–290.

Palache, C., Berman, H. and Frondel, C. (1951) The System of Mineralogy, Vol. 2, 7th Ed., John Wiley & Sons, New York, pp. 719–720.

Penfield, S. L. (1905) On crystal drawing. American Journal of Science, 169, 39–75.

Povarennykh, A. S. (1972) Crystal Chemical Classification of Minerals, Vol. 2, Plenum Press, New York, p. 538.

Shannon, R. D. and Prewitt, C. T. (1969) Effective ionic radii in oxides and fluorides. Acta Crystallographica, B25, 925–946.

Strunz, H. (1970) Mineralogische Tabellen, Akademische Verlagsgesellschaft, Leipzig, p. 311.

Von Knorring, O. (1963) VI(c) Report on mineralogical research. 7th Annual Report (1961-1962), Research Institute of African Geology, University of Leeds, 33–37.